Material Models for Polymers under Crash Loads Existing LS-DYNA Models and Perspective

Frank Huberth, Stefan Hiermaier, Marika Neumann

Fraunhofer Ernst Mach Institut (EMI), Freiburg, Germany

Abstract:

Continuum mechanical modelling of structures made from thermoplastic materials under crash loads including large deformations and failure is still challenge in the existing numerical tools for crash simulation. This challenge has two components. One is the fact that the micromechanical nature of the material must be modelled by continuum mechanical models. Continuum models, for pure or for reinforced plastics, will always get either very complex or not very precise if applied to macro molecular materials. The second challenge is the derivation of material parameters for these models by design and instrumentation of adequate experiments.

In this paper, an overview on existing material models for thermoplastics applicable on shell elements in LS-DYNA will be given. Specifically, the problem of parameter derivation from experimental data is discussed and examples will be given.

Based on a PHD thesis [1] a new approach is described with a special focus on the problem of dilatation under tensile loading.

Some perspectives for future developments are described and illustrated by examples.

Keywords:

Polymeres, Plastics, Thermoplastics, Crash Simulation, Impact, Material Modelling, Material Characterisation, Input Data, Material Parameters

1 Preface

Until some years ago, state of the art for impact and crash simulations of units and parts made from modern polymer materials was to apply material models originally developed for metals. To some aspects, this is still the case in nowadays practice. This contribution will take focus on thermoplastics in the wide area of polymer materials. An introduction to the topic should be given by this paper with some examples.

Application of thermoplastics in automotive parts is still increasing, with or without fillers or fibres. Surface grades can be produced that allow for application without additional finishing like painting or covering. Different ways for part production, combinations and innovative joining technology permit the design of parts with still increasing complexity. The pictures below show conventional carpeting for an A-pillar. This part includes a ventilation slot and rips as fortification for the case of a head impact. Simulation of parts like those, specifically with shell elements, is already a challenge.

Figure 1: A-pillar carpeting with lamellar fortification and ventilation slot [1]

In most cases the modelling for such parts will be done with shell elements in consideration of all the restrictions of shell elements. This proceeding is caused mainly by the needed computing time, not only for the component but rather for the full car model. The use of solids in such thin walled structures would decrease the time step and therewith increase the overall computing time breaking every limit.

OEMs (Original Equipment Manufacturers) in the automotive industry can dispose today of 1000 CPUs and more. This power allows already a very detailed model for smaller components but not for bigger problems yet. With a further increase of computing power and applications optimised for parallel computation the use of solids could be an option in the future. Since this is not yet possible, for the rest of this paper we will restrict ourselves to shell element formulations.

2 Overview of material models for polymers in LS-DYNA

As mentioned above, most material models available utilize approaches with the assumption of linear elasticity and an adjacent plastic regime including strain hardening. In addition, failure can be modelled by criteria in the stress, strain or mixed space. The well known model *MAT_024 (*MAT_PICEWISE_LINEAR_PLASTICITY) in LS-DYNA was often used for the crash and impact simulation with thin walled structures and is intensely used still today. This material model describes the elastic deformation as linear. For most thermoplastics a strain rate hardening can be observed (Figure 2). Strain rate effects are considered by shifting the yield stress. Analogous the pure elastic deformation increases with the strain rate. The plastic material behaviour can be described with stress- strain curves for different strain rates by a separate plastic strain part [2].

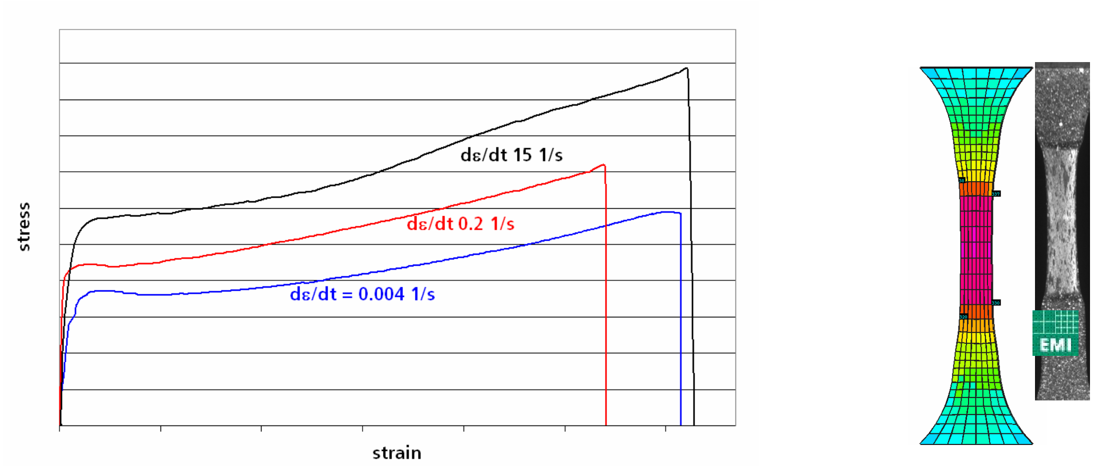

Figure 2: Stress-strain diagram for different tensile loading speeds and plastic sample deformation in the simulation and the experiment [3]

When using *MAT_024 for thermoplastic materials it is recommend to activate the viscoplastic option (VP=1) to improve the results and reduce oscillations also. This option was reformulated for Version 970 in 2003 [4].

Many Thermoplastics show a localisation of deformation (Figure 3). Due to this effect the geometric scale on which the determination of the stress-strain behaviour is performed plays a decisive role for the simulation. If the data provided for the material model is derived from a significantly different scale than the one of the discretization, no material model can reach a sufficient accuracy. An example for a PC-ABS with distinct localisation is shown below. The two curves show a stress-strain curve developing for different measurement lengths. This issue is treated in [1] and [3] in greater detail.

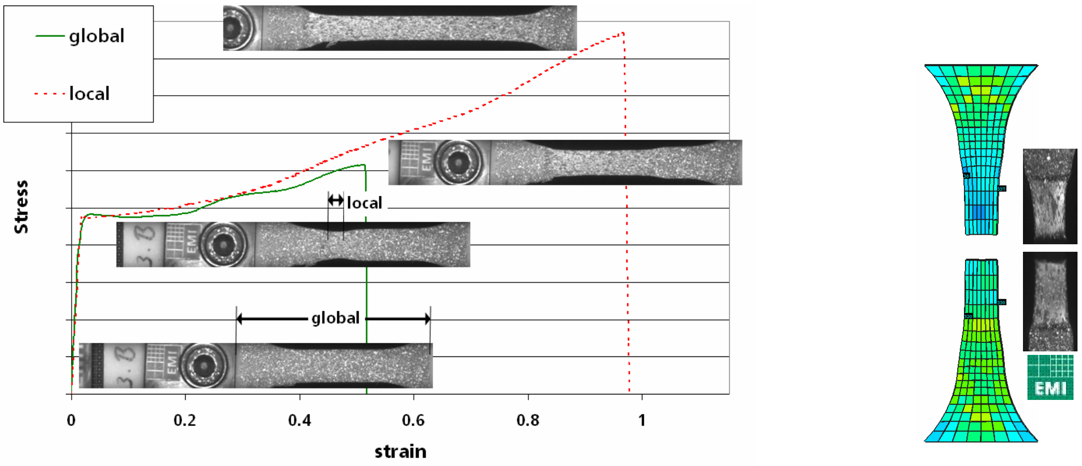

Figure 3: Stress-strain diagram for different measurement scales for two experiments and plastic sample deformation in the simulation and the experiment

Another restriction in many models are the criteria that cause element elimination (Figure 3). For *MAT_024 a maximum plastic strain criteria, a time step based element elimination and the possibility of a user defined failure subroutine as well as no consideration of failure are disposable. This appears to be sufficient but a user defined failure subroutine is not an option for the normal daily use and the maximum strain criteria only for more brittle failure behaviour.

The experimental determination of the one value for maximum plastic strain is not that easy in tensile tests for example as the results scatter frequently by more than 30% (Figure 2). Another point is the dependency of failure on strain rate and loading situation.

The strain rate influence on the failure strain is included in a material model, developed not for metals but for plastics, *MAT_089 (*MAT_PLASTICITY_POLYMER) [2]. This model represents an elastic-plastic material. The required stress-strain curve defines the elastic and plastic material properties; no separation of elastic and plastic parts is needed. This handling should help to simplify the parameter determination as for many thermoplastics appointing the yielding point is not distinct. Anyway, a determination of a so called yield stress depending on the strain rate is necessary to consider the rate dependent embrittlement. In the same manner, the rate dependent failure as maximum strain can be included. To avoid oscillations of the strain rate at high frequencies a low pass filter is available. A viscoplastic option (VP) is not provided. In comparison with *MAT_024 the only benefit of this model from a practical point of view is the possibility to include a rate dependent failure. The controllability for *MAT_024 offers the user more options.

Another model specifically developed for plastics is *MAT_101 (*MAT_GEPLASTIC_SRATE_200a). This model includes strain rate effects, different criteria for element elimination against strain rate, principal stress and plastic strain. A special feature is the definition of unloading moduli as a function of the plastic strain. Basis for the model is a stress-strain curve but additional parameters have to be determined, like the pressure sensitivity factor. As mentioned in [2], GE Plastics could provide related parameters for their materials. For other thermoplastics these parameters are not available in a wide range.

These two last models are not so extensive in use as the first one, *MAT_024. From the authors point of view one main reason for this is the comparatively easy handling and parameter determination for *MAT_024. For additional information it should be referred to [2].

A kind of successor of *MAT_024 is *MAT123 (*MAT_MODIFIED_LINEAR_PLASTICITY). The main disadvantage of *MAT_123 compared to *MAT_024 is the currently not used VP-option. The enhancements of *MAT_123 are additional failure options. The latest improvement is the inclusion of rate dependence of the plastic thinning failure.

*MAT_081 (*MAT_PLASTICITY_WITH_DAMAGE) is an elasto-visco-plastic material model that is comparable to *MAT_024 but includes an additional damage approach. Reaching a defined strain softening is introduced until material rupture. This softening should regard cavitation in the material under loading. Voids occur mainly under tensile loading but the model regards no different load cases.

Consideration of a load dependent material behaviour for tension and compression is given in *MAT_124 (*MAT_PLASTICITY_COMPRESSION_TENSION). This model offers the user the possibility to define yield stresses for tension and compression separately. The elastic constants are identical for both. Strain rate effects are modelled by a Cowper-Symonds [2] model. The separated consideration of tension and compression could be useful for bending dominated loading cases.

For pure elastic problems a viscoelastic material model could be used. The only one available for shells is *MAT_076 (*MAT_GENERAL_VISCOELASTIC). An extensive explanation to the use of *MAT_076 is given in [5].

3 How to determine input parameters

All models are based on reliable data with a traceable extraction from material tests. For analytical models the extraction is a complex way with different steps of optimisation. The optimisation depends on the weighting of the different dependencies. The example shown below for a generalised Cowper-Symonds law gives an impression of the iterative nature of that kind of optimisation process (Figure 4).

The basic analytical plastic stress-strain curve for an artificial strain rate 0 is the base for the analytic evaluation of curves for other strain rates. The optimisation can be done by using software like LS-OPT. The strain rate dependency can only be approximated; its accuracy will always be restricted to a certain range, that should be given together with the measured data. Other analytical models are based on the Gísell model for example [6]. Advantages in calculation time for analytical models over look up tables can be more and more neglected nowadays.

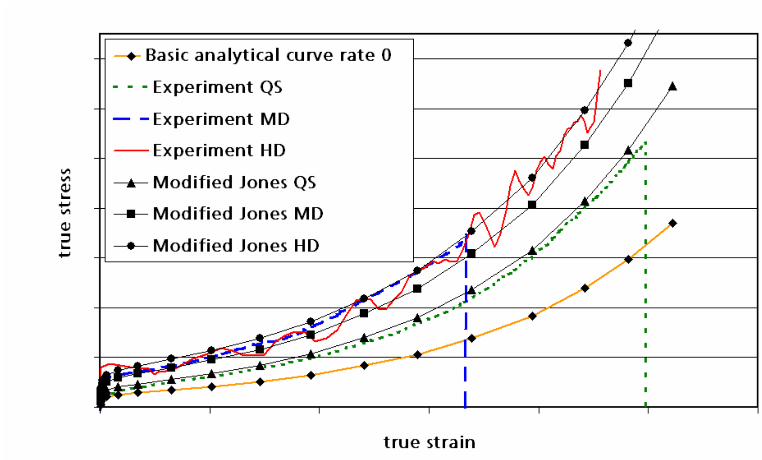

Figure 4: Stress-strain diagram for different strain rates and an itterativ determined basic curve for an analytical model (Modified Jones for PAM-CRASH)

The direct method is offered by tabulated material models like *MAT_024. The experimental data can be used with minimal adaptation. For *MAT_024 for example, the elastic constants have to be evaluated and the yield points for the different strain rates need to be determined.

However, as mentioned already, the determination of the yielding point is a problem since it is not distinct for many thermoplastics. *MAT_024 uses a linear elastic approach. Thus, the nonlinearity in the elastic part cannot be modelled. It is recommended to keep the total curve steady and to provide a smooth transition to plasticity (Figure 5). Often this aim is reached by permitting plastic deformation in the model by a lowered yield strains. The second step is the separation of elastic and plastic shares of the strain data. This depends on the constant Youngís modulus and the actual stress. The separated plastic stress-strain curves for the different strain rates can be represented by a reduced number of points and smoothed especially for higher strain rates where the experimental data show in most cases significant oscillations. An extrapolation should be done beyond the defined failure strain. The experimental data is generated by tensile tests in most cases. These tests are mainly performed at constant velocity but not at constant strain rate. In [1] an interpolation has been performed to generate curves for constant strain rates. In figure 6 an approach is shown that uses polynomial interpolation to generate curves of constant strain rate. The interpolation of data coming from different tests with varying strain rates during the tests uses the implicit assumption that there was a unique relation between stress, strain and strain rates. In other words, history effects are neglected. However, this approach allows the user to generate sets of curves with constant strain rates.

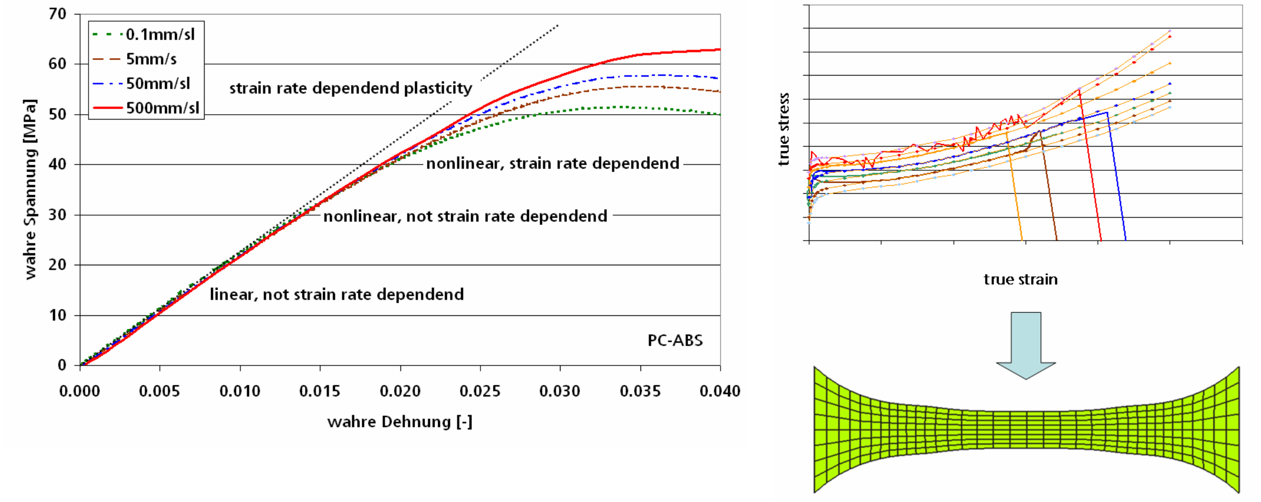

Figure 5: Stress-strain diagram for different strain rates until plastic deformation occurs (left) and with extrapolated input curves of stress and plastic strain (right)

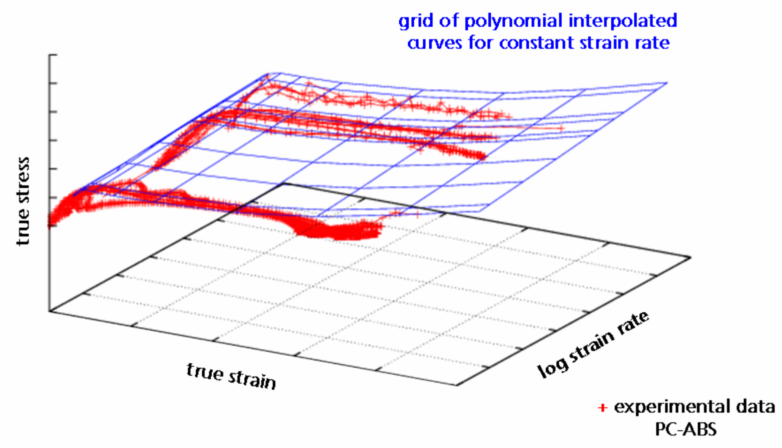

Figure 6: Stress-strain diagram for different strain rates

As mentioned above, the problem of experimental determination of maximum plastic strain values is that the results show a large scatter. A sufficient number of tests have to be performed to allow an approximately statistical analysis. If a degradation model is used, the testing efforts will multiply.

An ISO standard ìPlastics -- Determination of tensile properties at high strain ratesî is under development [ISO/DIS 18872]. From the authors point of view this standard will not cover the necessities for the modelling of plastics in crash applications. EMI develops a test procedure based on the experience in this field of work with special regard for material modelling. This work is done for the FAT (German Association for Research in Automobile Technology) with support of German OEMs, software suppliers, automotive suppliers and plastic producers. This standard will be extendable as the evolution of enhanced material models will progress. Up to now, different basic material models for LS-DYNA and PAM-CRASH are investigated. An integration of a database for crash simulation in CAMPUS [7] for the future is already under discussion.

4 Recent developments

In the year 2002 a PHD-Thesis with to the topic charakterisation and modelling of unreinforced thermoplastics for numerical simulation of crash [1] has been concluded by Michael Junginger at EMI. He developed a material model that included a stress state dependency for tension, compression and shear (Figure 6). Strain rate and temperature were also considered.

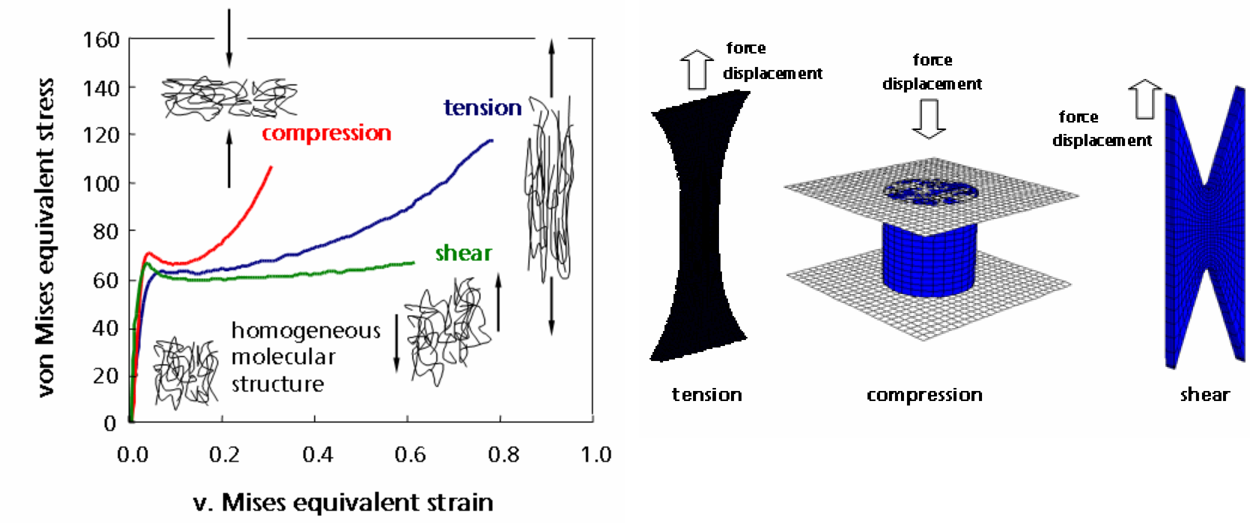

Figure 6: Stress-strain diagram for different loadings (left) and the models of the test setups (right)

The elastic deformation was considered as linear and defined by the Youngís modulus and the Poissonís ratio. This simplification was accepted since the energy absorption by the plastic deformation was in the focus of the work.

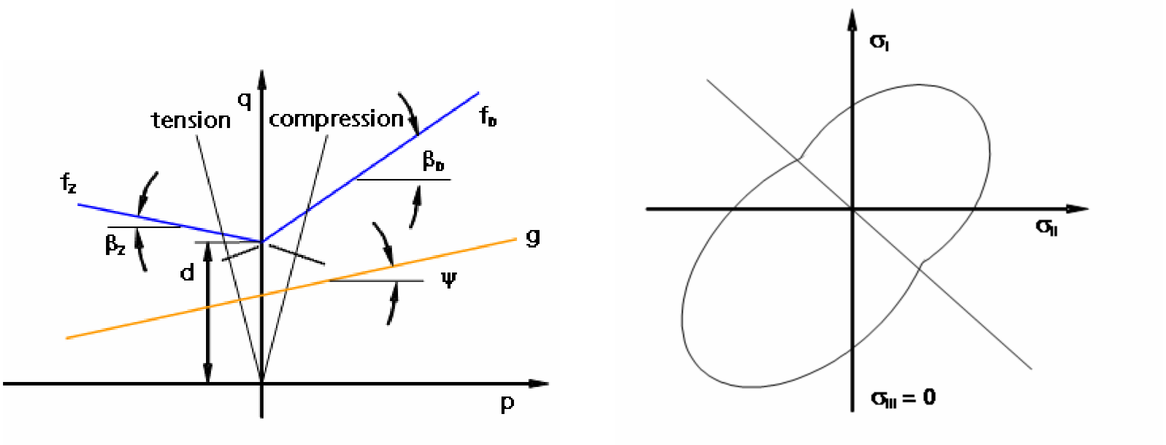

Figure 7: Schematic evaluation of the yield potential (fx) and the plastic potential (g) for tension, compression and shear (p=0) in the deviatoric plane (left) and a sketch of the resulting yield surface for a plane stress state (right)

The model bases on the assumption of linear elastic behaviour and uses a non associated flow rule. To take account for the micromechanical influence of different molecular deformation processes under different stress states an anisotropic hardening was modelled by yield potentials for tension, compression and shear as:

$$f\left(I_1, J_2, \beta_Z, d, \bar{\varepsilon}^{pl}\right) = q - p \tan \beta_Z\left(\bar{\varepsilon}^{pl}\right) - d\left(\bar{\varepsilon}^{pl}\right) \quad \text{for } p \le 0 \tag{1}$$

$$f\left(I_1, J_2, \beta_D, d, \bar{\varepsilon}^{pl}\right) = q - p \tan \beta_D\left(\bar{\varepsilon}^{pl}\right) - d\left(\bar{\varepsilon}^{pl}\right) \quad \text{for } p > 0 \tag{2}$$

Where
I_1: first Invariant of the Cauchy stress tensor
J_2: second Invariant of the deviatoric stress parts
$\beta_{Z/D}$: friction angles for shear-tension ($_Z$) and shear-compression ($_D$)
d: cohesion (3)
$\bar{\varepsilon}^{pl}$: equivalent strain (v. Mises)
p: hydrostatic stress part
q: deviatoric stress part

A logarithmic strain rate and linear temperature dependency was considered and described based on the Bauwens and Bauwens-Crowet model [10]. The cohesion d is described as follows:

$$\frac{d}{T} = A_\alpha \left(\ln 2C_\alpha \dot{\bar{\varepsilon}}^{pl} + \frac{Q_\alpha}{RT} \right) + A_\beta \sinh^{-1}\left(C_\beta \dot{\bar{\varepsilon}}^{pl} \exp \frac{Q_\beta}{RT} \right). \tag{3}$$

$A_{\alpha,\beta}$, $C_{\alpha,\beta}$ and the activation energy for molecular movement $Q_{\alpha,\beta}$ represent material parameters. Additional explanations for the parameters are given in [1].

The resulting model is able to reproduce volume increase (dilatation) as $\Psi>0$ is provided. This is one of the main disadvantages over the models described in chapter 3 that are all based on the assumption of constant volume as it is done for v.Mises.

Some tests were performed recently at EMI to estimate the dilatation under tensile load. Two optical measurement systems were used to determine the tensile strain, thickness reduction and the lateral reduction (Figure 8). These measurements were performed locally during the tensile test. The samples were machined out of plate material.

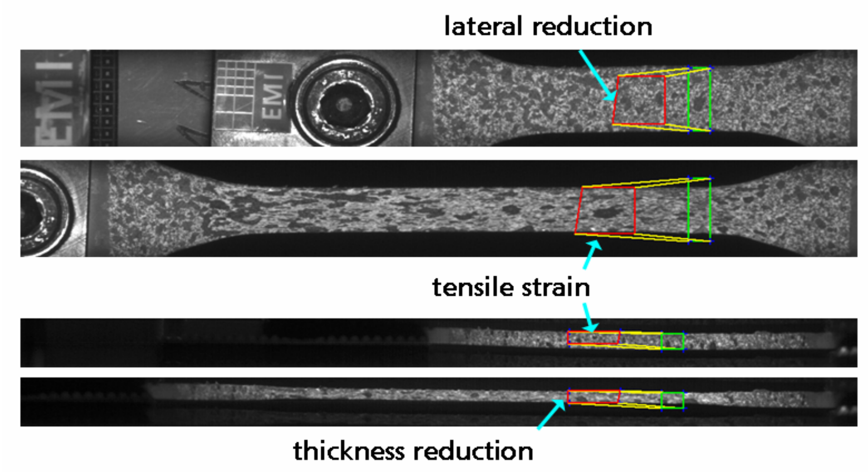

Figure 8: Optical determination of the segment volume assuming a prismatic segment

The analysis of the segment volume leads to an increase in volume up to more than 30% for quasi static loading. The two materials diagrammed below show different characteristics during tensile tests. The PC-ABS shows significant necking (Figure 9). The PA-ABS shows a more uniform deformation (Figure 10). This leads to the different curves. For the PC-ABS the main dilatation occurs during the necking phase, for the PA-ABS it is more uniform.

For comparison, an analysis for the assumption of a constant thickness is displayed (Figure 9, 10). The difference between the two approaches shows the necessity to measure the thickness evaluation.

Not shown is the not obvious difference for a local and a global strain measurement for the PA-ABS. During the tensile tests also for the PA-ABS localisation has been determined. These zones change during the deformation process. For the analysis the area of the first localisation has been chosen.

The scales of the segments for both materials are equal.

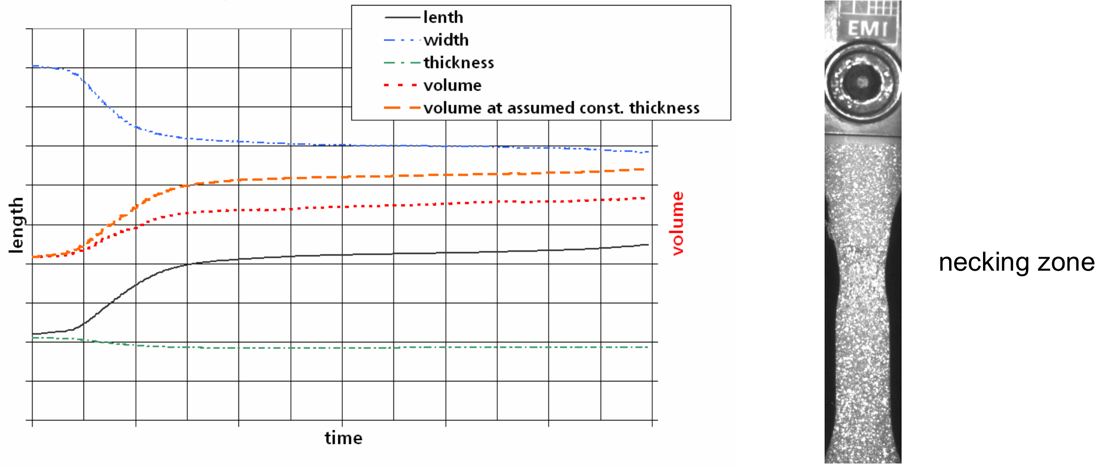

Figure 9: Volume evaluation for a PC-ABS (left) and deformation under tensile loading with necking zone (right)

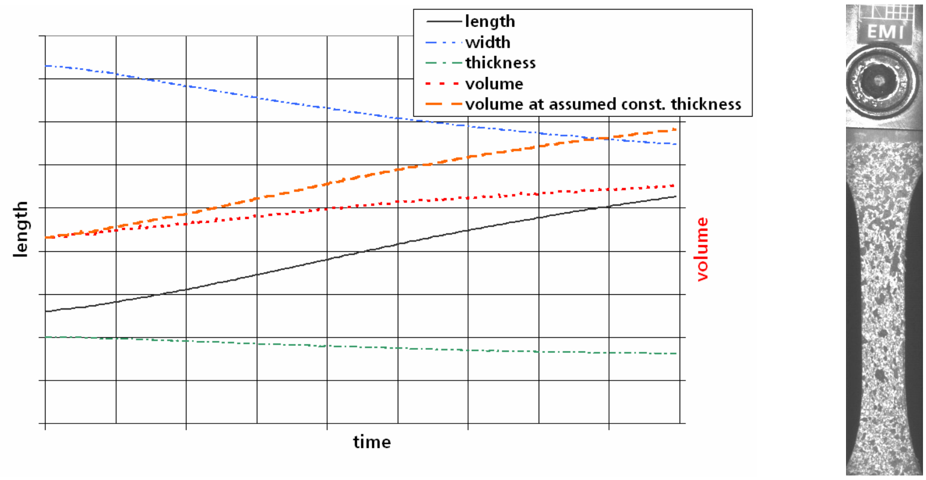

Figure 10: Volume evaluation for a PA-ABS (left) and deformation under tensile loading (right)

A comparable approach for plastic material models in LS-DYNA was developed in 2005 by Haufe, Kolling, Feucht and DuBois for LS-DYNA [8, 9].

5 Future challenges in crash simulations of plastic components

5.1 Welding lines and joining zones

Thermoplastic and thermo sets as well give a multitude of design options, possibilities of part and function integration and material mixing. During the production process in some areas weakening can occur, for example as two melting fronts get together a welding line is build. This is an area of different material behaviour, generally a weaker one. Other points are marks from the mouldings. Examples for these two phenomena are pictured in figure 11. A semi spherical impactor comparable to a head impactor according to WG 17 is accelerated on a flat circular specimen. Analogous the particularities of the different specimen different failure can be observed. Cracks are build up along the welding line (Figure 11 left, 12 left) next to the mark or for a more homogenous specimen(Figure 11 centre) in the clamping zone were complex stress-strain states result of the loading case (Figure 11 right). The last case can be reproduced numerically with a relative simple shell model. The two other cases would need additional work. The welding line for example could be considered by lines of elements with changed material parameters. And the moulding mark could be modelled by a mesh adoption and an adapted thickness.

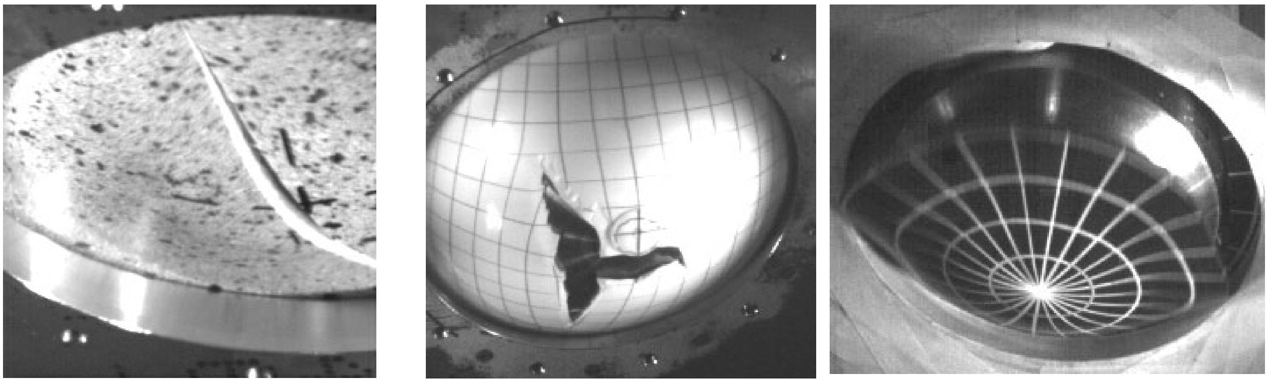

Figure 11: Ball intrusion test for a PC_ABS with welding line (left), ejector mark (centre) and a PP-TV(right)

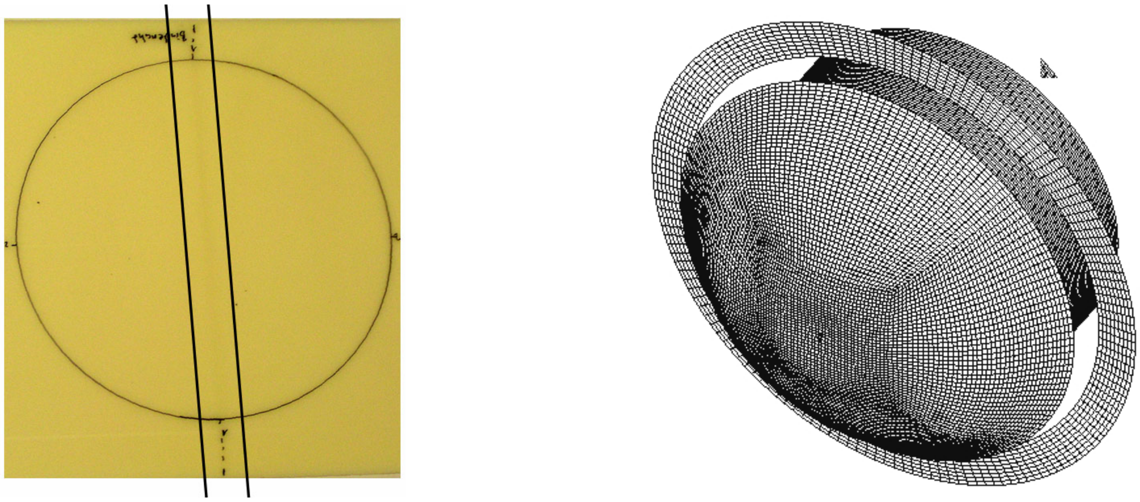

Figure 12: Sample plate for the ball intrusion (PC_ABS) with a welding line between the black marks (left) and a failure optimised simulation of a test for PP-TV (right)

5.2 Rips and cross ribs modelled with shell elements

Very often rips of all kinds are used in plastic components to provide stiffness in lightweight structure. Because of demoulding these rips have always an increasing thickness from the top edge to their bottom. For the shown simulation (Figure 13) the thickness is accepted by a stepwise increasing shell thickness. This is of course influenced by the element dimension. At the bottom of the rip the DOF (degrees of freedom) are reduced. The rotations at these nodes are blocked. This effort should include the radius at the bottom of the rip.

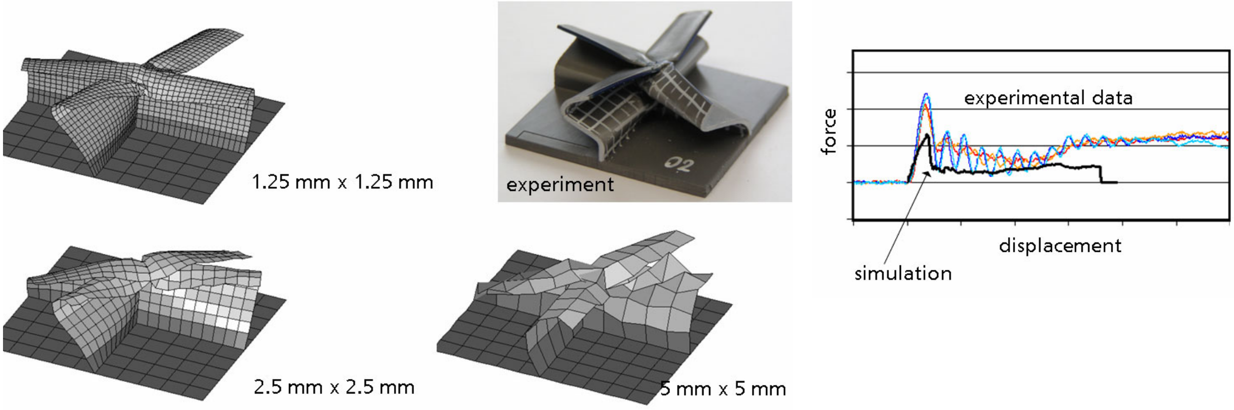

Figure 13: Cross ripped sample after a dynamic compression test experiment and 3 different models with 3 element sizes (left), measured an calculated (1.25 mm) force-displacement curves (right)

The deformation is in comparison to the experiment quiet good reproduced with increasing accordance for smaller element dimensions. The displayed element dimensions could be used for head impact scenario. Here the user is given the possibility to refine the mesh in the impact zone because of this local loading situation. Having regard to the number of head impact scenarios that have to be under examination this handling seems not practicable.

Although the deformation is reproduced quiet well the force level in the simulation is constantly below the measured curves. Only the first rising shows a sufficient agreement. The simulated curve evaluation indicates to early failure and an overestimated softening of the structure due to the failure.

5.3 Process chain and coupling with crash analysis

The examples pictured in figure 12 give an impression about the influence of the manufacturing process. Recently the production process finds more and more consideration for fibre reinforced thermoplastics. Here the anisotropy is defined by the fibre orientation that is driven by the moulding process [10]. The interfaces between the tools for mould flow analysis or other production process simulations and the crash codes have to be developed or enhanced. In most cases the mesh must be mapped. For injection moulded parts for example from a fine triangular shell mesh to quadrilateral dominated mesh for the structural analysis. The wall thickness has to be mapped afterwards. Here a lot of improvement can be done in the future comparable with the developments for metals, where you find interfaces to sheet metal forming or welding and casting for example.

5.4 Durability and crash analysis

The durability and impact or crash interaction is a field for future work. Impact loadings will definitely affect the durability by changing the fatigue strength for example. And contrary the loading history of a part will show an influence on the crash behaviour. Compressive strength can lead to higher impact resistance or crack growth and damage can cause a structural collapse after a non critical impact. This will be a field of research for the future. First the coherences have to be investigated. Afterwards an estimation for the modelling options will be possible.

5.5 Aging and degradation

Like for the interaction of durability and impact the effects of aging will be a field of research for the future. One main problem here is to analyse first the main aging processes for the materials. This could differ very strong. Up-to-date an additional material characterisation will be performed for aged material to determine new material parameters. This is a possible procedure for the interaction of durability and crash too. This is restricted for one constellation of aging or loading history and impact.

6 Conclusions

There is a big variety of material models with individual restrictions available in LS-DYNA and other crash simulation codes. A good basis model has been developed by Junginger that allows for simulation of anisotropic elastic-plastic behaviour including strain rate and temperature dependencies. A major advantage over other models is the option to model volume dilatation. The necessary next step is a failure model with predictive capabilities. The latest developments have to be implemented in the code and tested in the practical work.

On main topic for the future could be the regard of the process chain for the structural analysis overall.

7 Acknowledgements

Most of the work that was done through the last years and provided the results and conclusions shown in this paper was sponsored by the FAT (German Association for Research in Automobile Technology) with support of German OEMs, software suppliers, automotive suppliers and plastic producers. The continuity of discussions, tests and related model developments turned out to be a very fruitful base for improvements of the numerical tools needed so much.

8 Literature

[1] Junginger, M., Hrsg. Thoma, K.: " Charakterisierung und Modellierung unverst‰rkter thermoplastischer Kunststoffe zur numerischen Simulation von Crashvorg‰ngen", Schriftenreihe Forschungsergebnisse aus der Kurzzeitdynamik, Heft Nr. 3, Freiburg/Brsg. 2004, ISBN 3-8167-6339-1 Fraunhofer IRB Verlag

[2] LSTC: "LS_DYNA KEYWORD USERSíS MANUALì, Version 970, 2003

[3] Huberth, F., Thoma, K.: ìVon der Werkstoffpr¸fung zum Kopfaufschlag Aus Kennwerten entsteht ein Modellì 3rd CTI Conference Pedestrian Protection, Innovativ Developments and Attempts, Frankfurt 2004

[4] ìFEA Informationsì December 2003

[5] DuBois, P.:ìWorkshop on Crshworthiness Simulationì, 22nd CAD-FEM Usersí Meeting, Dresden, 2004

[6] Milcent, G.:îEvaluation of constitutuive laws of plastic materials for crshwortiness simulationsî, EuroPAM2004, Paris

[7] http://www.campusplastics.com/

[8] Kolling, S., Haufe, A., Feucht, M., DuBois, P.:ìA Viso-plastic Material Model with Damage for Thermoplasticsî, 10. Problemseminar ìDeformation und Bruchverhalten von Kunststoffenî, Merseburg 2005

[9] Haufe, A., DuBois, P., Kolling, S., Feucht, M.,:ìA semi-analytical model for polymerssubjekted to high strain ratesî, 5th European LS_DYNA Users Conference, Birmingham, 2005

[10] Krivachy, R.: ìCrashsimulation an faserverst‰rkten Kunststoffenî, Otti-Profiforum Wirtschaftlicher konstruieren mit LFT, Regensburg, 2005

[10] Bauwens-Crowet, C., Bauwens, J.-C., Homes, G.: The Temperature Dependence of Yield of Polycarbonate in Uniaxial Compression and Tensile Tests. *Journal of Materials Science*, 7 (1972) 176-183